Eur. Polym. J. Vol. 27, No. 7, pp. 573–579, 1991
Printed in Great Britain.

0014-3057/91 $3.00 + 0.00

DETERMINATION OF REACTIVITY RATIOS FOR THE ANIONIC COPOLYMERIZATION OF ETHYLENE OXIDE AND PROPYLENE OXIDE IN BULK

FRANK HEATLEY,[1]* GA-ER YU,[1] COLIN BOOTH[1] and TREVOR G. BLEASE[2]
[1]Department of Chemistry, University of Manchester, Manchester M13 9PL, England
[2]ICI Chemicals and Polymers Ltd, P.O. Box 90, Wilton, Teeside TS6 8JE, England

(Received 23 August 1990; in revised form 26 October 1990)

Abstract—Reactivity ratios have been determined for the anionic copolymerization of ethylene oxide and propylene oxide in bulk over the temperature range 0–80°C. The ratios were obtained by two methods, the first using the variation of copolymer composition with monomer feed composition according to the Mayo–Lewis equation, and the second using the triad sequence distribution derived from ^{13}C-NMR spectra. In both methods, the ratios were obtained by a computer search for the values giving the best fit between simulated and experimental data. The program took composition drift into account by numerical simulation of the copolymerization as a series of small steps, the feed composition being adjusted after each step. The reactivity ratios were independent of temperature within experimental error, with average values $r_E = 2.8 \pm 0.6$ and $r_P = 0.25 \pm 0.07$ from the Lewis–Mayo equation, and $r_E = 3.1 \pm 0.4$ and $r_P = 0.30 \pm 0.04$ from the triad distribution.

INTRODUCTION

Statistical and block copolyethers have applications in many areas, for instance as hydraulic fluids, water-soluble polymers, surfactants and polymer electrolytes. The development of techniques for characterizing the chain structure of these materials is of considerable importance, as is the development of a detailed understanding of the chemistry involved in their production. We have recently published several papers on the use of NMR in characterizing the composition, end-group structure and sequence structure of homopolymers of propylene oxide (PO) [1, 2], 1,2-butylene oxide [3] and styrene oxide [4], and of their copolymers with ethylene oxide (EO). However information on the mechanism of copolymerization, for example reactivity ratios, is limited. Table 1 summarizes data on reactivity ratios for the anionically catalysed copolymerization of EO and PO, the subject of this paper. There is broad agreement that $r_E > 1$ and $r_P < 1$, consistent with a greater reactivity of EO compared to PO. However the quantitative agreement is poor, even for systems in similar physical states and with similar catalysts, e.g. the bulk copolymerizations catalysed by potassium glycerate/glycerol, anhydrous KOH and potassium methoxide. The discrepancies are probably due to differences in experimental conditions, analytical techniques and data reduction methods. In two cases [5, 8], information on experimental methods is unfortunately not readily accessible. Stolarzewicz *et al.* [6] carried out the reaction at atmospheric pressure using a pressure-equalized reflux condenser to recirculate the monomers. The polymerization was followed by gas chromatographic analysis of the monomer feed, but it is not clear at what point in the recirculation this analysis was made, nor how the actual feed composition at the copolymerization site was determined. Rastogi and St Pierre [9] used elemental analysis to determine the copolymer composition. However this method is not very precise since the difference in elemental weight % between PEO and PPO homopolymers is quite small (for example, the weight % of carbon in PEO is 54.55%, in PPO, 62.07%). Gladkovskii and Ryzhenkova [13] did not use the conventional method of correlating copolymer composition with feed composition, but attempted to determine individual rate constants for the four distinct propagation reactions by measuring the rates of the reactions of the potassium salts of $CH_3OCH_2CH_2OH$ or $CH_3OCH_2CH(CH_3)OH$ with EO or PO. However it is not clear how much the measured rates are affected by further propagation steps after the first addition to the initiator. Boussias [11] and Ponomarenko *et al.* [12] used ^{1}H-NMR to determine the copolymer composition, but the instrumentation was of the older continuous-wave type which lacked the ability to make the off-line baseline corrections necessary for accurate intensity measurements.

In view of the lack of accurate data, we have carried out a systematic study of the anionic copolymerization of EO and PO in bulk over the temperature range 0–80°C using the potassium or sodium salt of 1-methoxy-2-propanol as initiator. The conversion was limited to < 10% in order to minimize drift of the monomer feed composition, and the amount of initiator added was adjusted to give molecular weights of at least 6000 at 10% conversion in order to minimize the effects of chain-ends on the monomer sequence distribution. The reactivity ratios were obtained by two methods, the first using the variation of copolymer composition with monomer feed composition according to the Mayo–Lewis equation, and

*To whom all correspondence should be addressed.

Table 1. Reported reactivity ratios for the anionically catalysed copolymerization of EO and PO

Ref.	T (°C)	r_E	r_P	Initiator and catalyst	Solvent	Analytical and calculation methods
5	70	3.0	0.17	?	Bulk?	?
	90	2.5	0.26	?	Bulk?	?
6	120	1.6	0.36	Potassium glycerate/glycerol	Bulk	^{13}C-NMR Heublein method [7]
8	?	4.04	0.16	?	?	?
9	25	6.5	0.5	Anhydrous KOH	Bulk	Elemental analysis Fineman–Ross [10]
11	25	1.34	0.49	KOMe	Bulk	^{1}H-NMR Fineman–Ross
12	70	2.35	1.49	Sodium phenolate	?	^{1}H-NMR Fineman–Ross
13	60	3.7	0.17	Potassium alkoxide	Chlorobenzene	From rate constants
	95	4.8	0.14		benzene	

the second using the triad sequence distribution derived from ^{13}C-NMR spectra as described in Ref. [1].

EXPERIMENTAL PROCEDURES

NMR spectroscopy and GPC

^{1}H- and ^{13}C-spectra were obtained using a Bruker Spectrospin AC300E spectrometer operating at 300 MHz for ^{1}H and 75.5 MHz for ^{13}C. Solutions in $CDCl_3$ contained 200–400 mg polymer per cm^3 solvent. The copolymer composition was determined from both ^{1}H- and ^{13}C-spectra using a pulse interval of at least 12 sec in order to allow complete relaxation between pulses. The ^{13}C-spectra were ^{1}H-decoupled throughout the acquisition, as a trial experiment showed that the EO and PO components had identical nuclear Overhauser enhancements close to the maximum value of 2.988. The triad sequence distribution was determined from ^{13}C-CH and -CH_2 subspectra as described in Ref. [1]. The subspectra were obtained by respectively adding and subtracting DEPT spectra [14] obtained with final ^{1}H-pulses of 45° and 135° flip angles. The weighting of each spectrum was adjusted empirically in order to null resonances known to be entirely of the undesired multiplicity.

Materials

EO (Fluka, >99.8%) was transferred from a cylinder into a flask cooled in a solid-CO_2/acetone bath, and distilled through a vacuum line into a second flask containing CaH_2 where it was stirred at 0°C for at least 10 hr (monomer: $CaH_2 \approx 10:1$). It was then distilled at least twice from CaH_2 powder, and again 2 hr before use.

PO (BDH, >99.5%) was stirred over CaH_2 for at least 8 hr at room temperature before distillation through a column of KOH pellets and collection of the middle cut over CaH_2. It was then treated in the same way as the EO.

It was observed that sometimes the monomers slowly polymerized on storage over CaH_2, probably because of slight hydrolysis of the hydride to give hydroxide which acts as initiator. This process was unimportant as the monomers were always redistilled through the vacuum line immediately before use.

Preparation of initiating solution

Polymerization was initiated by the potassium or sodium salt of 1-methoxy-2-propanol (MP, Aldrich, 98%). MP was dried ($MgSO_4$) before distillation and retention of a middle cut. Potassium or sodium metal was cut and weighed under dried petroleum ether, and added directly (under dry N_2) to the dry MP at a mole ratio of *ca* 1:3 (metal:MP). Usually a freshly prepared initiator solution was used. Stored initiator solution could be successfully used provided it remained colourless or, if concentrated, cloudy-white at room temperature. Discoloured (brown) solutions could not be used. The concentration of salt in the prepared solutions (colourless at 100–150°C, cloudy at room temperature) was 3–4 mol dm^{-3}.

Copolymerization

Copolymerizations were carried out in ampoules (11 mm i.d., *ca* 20 cm long) sealed by a teflon tap. For copolymerizations at 40°C and below, the ampoule was flushed with dry N_2 and the required amount of initiator solution (typically 10 μl) was injected into the ampoule by a micro-syringe. The ampoule was attached to the vacuum line and the excess of MP removed by evaporation under vacuum at about 120°C (heated by hot-air blower). The monomers were then distilled into sealed tubes (containing a small quantity of dried molecular sieves) and from there known volumes of each

Table 2. Characterization data for the copolymers

T (°C)	Sample No.	Conversion (%)	$\bar{M}_n \times 10^{-3}$	f_E(initial)	F_E
Potassium salt initiation					
0	34	3.6	7.8	0.160	0.401
	35	6.5	10.5	0.334	0.633
	36	4.4	9.0	0.550	0.795
	37	8.3	12.5	0.756	0.906
	38	6.2	9.5	0.912	0.968
23	29	4.5	7.0	0.164	0.397
	30	7.0	10.0	0.389	0.651
	31	4.3	9.7	0.609	0.825
	32	4.2	7.2	0.711	0.880
	33	6.2	8.5	0.900	0.960
40	11	7.8	6.5	0.121	0.316
	17	7.5	6.8	0.412	0.660
	12	10.5	10.5	0.569	0.796
	16	9.5	11.5	0.717	0.886
	18	10.5	9.0	0.838	0.935
60	28	7.9	6.1	0.159	0.372
	39	6.3	8.3	0.411	0.669
	19	5.8	8.5	0.445	0.710
	41	7.1	11.0	0.538	0.774
	20	6.4	10.0	0.634	0.839
	40	6.7	10.5	0.709	0.875
	21	10.9	10.0	0.790	0.916
	22	8.5	7.2	0.906	0.964
80	23	5.9	5.0	0.169	0.394
	42	5.8	11.0	0.369	0.621
	24	8.0	7.2	0.374	0.636
	44	5.2	9.5	0.558	0.784
	25	9.4	8.2	0.561	0.785
	43	7.9	10.0	0.747	0.896
	26	16.1	10.0	0.749	0.891
	27	12.6	9.7	0.894	0.956
Sodium salt initiation					
40	45	1.0	3.2	0.242	0.537
	49	5.0	9.9	0.341	0.619
	46	3.7	11.0	0.507	0.765
	50	3.0	10.8	0.573	0.799
	47	3.1	14.4	0.616	0.835
	51	3.3	15.3	0.792	0.921
	48	2.7	9.9	0.831	0.937

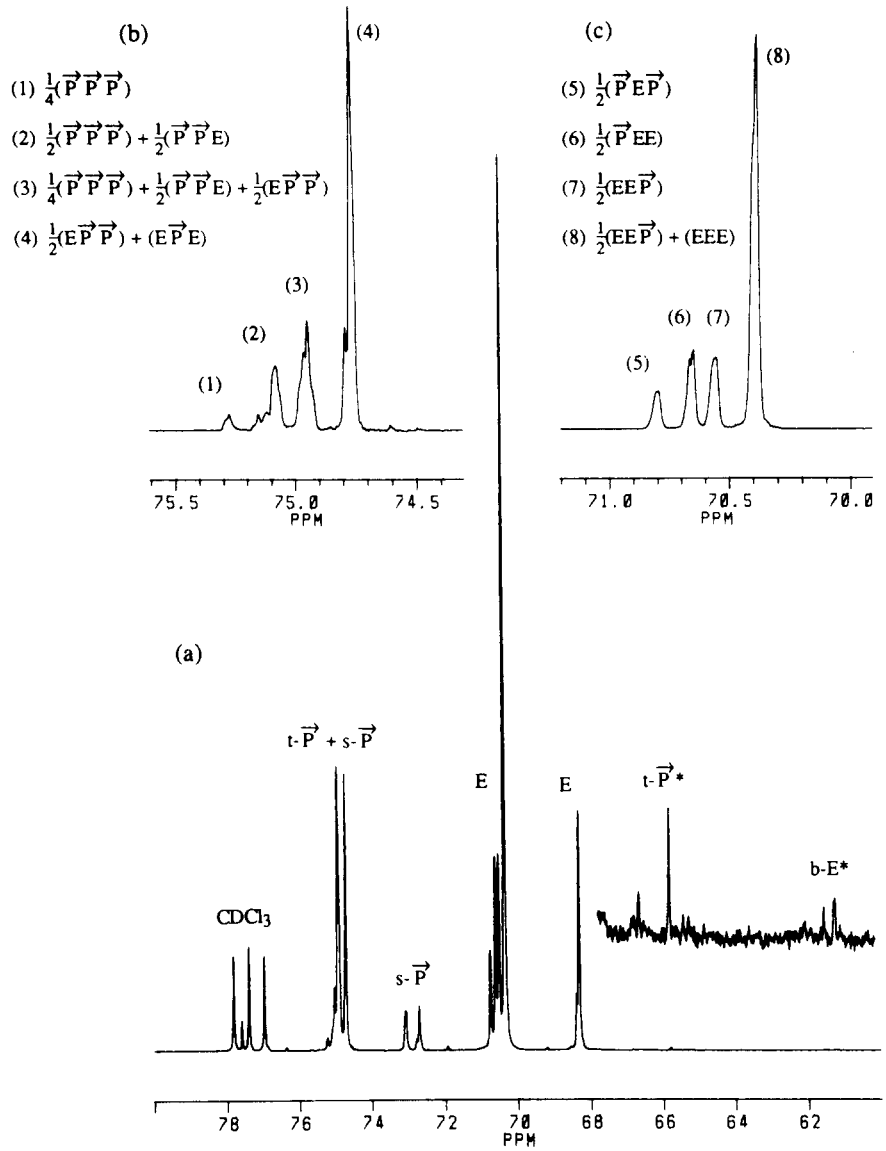

Fig. 1. ^{13}C-NMR spectrum of sample 30. (a) Backbone carbon spectrum; (b) CH subspectrum of t-$\vec{P}$ carbons; (c) CH_2 subspectrum of part of E carbon resonances.

were distilled into the ampoules, each ampoule being weighed after each addition. The total weight of monomers was typically 10 g. Finally the ampoule was well shaken to mix the contents, before immersing it in a water bath at the required temperature. From time to time, the level of liquid in the ampoule was measured and the conversion estimated volumetrically.

For the polymerizations at 60 and 80°C, the ampoule was equipped with a side-arm into which the initiator solution was placed. The monomer mixture could then be heated to the desired temperature before mixing with the initiator, so that the polymerization all took place at that temperature. This precaution was necesary because of the increased rates of reaction encountered at the higher temperatures.

DETERMINATION OF REACTIVITY RATIOS

Method I. Polymer composition as a function of feed composition

This approach is based on the conventional scheme of four propagation reactions with rate constants dependent on the terminal unit (denoted by *) and the adding monomer:

$$\ldots E^* + E \rightarrow \ldots E^* \quad \text{rate constant} \quad k_{EE}$$

$$\ldots E^* + P \rightarrow \ldots P^* \qquad k_{EP}$$

$$\ldots P^* + E \rightarrow \ldots E^* \qquad k_{PE}$$

$$\ldots P^* + P \rightarrow \ldots P^* \qquad k_{PP}$$

Table 3. Best-fit reactivity ratios from the composition data in Table 2 (Method I)

T (°C)	Counterion	r_E	r_P	RMS error (%)
0	K^+	3.0	0.25	0.38
23	K^+	2.8	0.25	0.82
40	K^+	2.8	0.25	1.10
60	K^+	2.9	0.28	0.50
80	K^+	2.7	0.26	0.83
40	Na^+	2.8	0.21	0.86

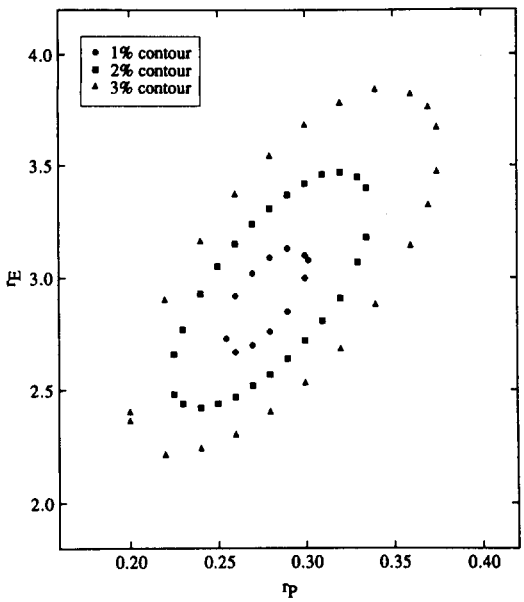

Fig. 2. Contour plot of the error sum R [equation (3)] as a function of r_E and r_P for the samples prepared at 60°C.

The instantaneous mole fraction of EO entering the copolymer, F_E, is expressed as a function of the mole fraction of EO in the monomer feed, f_E, by the Mayo–Lewis equation [15–17]

$$F_E = \frac{(r_E - 1)f_E^2 + f_E}{(r_E + r_P - 2)f_E^2 + 2(1 - r_P)f_E + r_P} \quad (1)$$

where r_E and r_P are the reactivity ratios defined by $r_E = k_{EE}/k_{EP}$ and $r_P = k_{PP}/k_{PE}$. This equation can be re-arranged to give the Fineman–Ross equation [10]

$$\frac{f_E(1 - 2F_E)}{F_E(1 - f_E)} = r_P + \left[\frac{f_E^2(F_E - 1)}{F_E(1 - f_E)^2}\right] r_E \quad (2)$$

(or an alternative version with the suffixes E and P exchanged). A plot of the appropriate functions of F_E and f_E should yield a straight line from which r_E and r_P may be obtained from the slope and intercept provided that two criteria are fulfilled:

(i) r_E and r_P are independent of the feed composition;
(ii) the conversion is sufficiently low for the instantaneous feed and copolymer compositions to be equated to the initial feed composition and the observed copolymer composition respectively.

If the second criterion is not met, integrated forms of the Mayo–Lewis equation should be used [18].

These algebraic methods tend to exacerbate experimental errors because of the transformation of basic experimental data (F_E, f_E) into more complex functions such as the left-hand side of equation (2). To avoid this problem, we adopted a simple numerical approach which involved a computer search for the values of the reactivity ratios giving the best-fit

Table 4. Triad probability distributions

Sample	EEE	EE$\bar{P}$	$\bar{P}$EE	$\bar{P}$E$\bar{P}$	E$\bar{P}$E	E$\bar{P}\bar{P}$	$\bar{P}\bar{P}$E	$\bar{P}\bar{P}\bar{P}$
34	0.052	0.097	0.096	0.156	0.106	0.138	0.126	0.229
35	0.230	0.157	0.151	0.096	0.156	0.073	0.083	0.054
36	0.495	0.133	0.133	0.034	0.136	0.029	0.035	0.005
37	0.741	0.083	0.075	0.008	0.078	0.009	0.007	0
38	0.907	0.029	0.031	0.001	0.029	0.001	0.002	0
29	0.052	0.097	0.096	0.152	0.109	0.138	0.134	0.222
30	0.272	0.151	0.150	0.078	0.160	0.080	0.073	0.037
31	0.555	0.127	0.118	0.025	0.118	0.028	0.024	0.004
32	0.679	0.093	0.095	0.013	0.094	0.013	0.011	0.002
33	0.889	0.033	0.036	0.001	0.036	0.002	0.002	0
11	0.024	0.070	0.068	0.154	0.078	0.158	0.121	0.328
17	0.287	0.151	0.150	0.071	0.162	0.075	0.073	0.031
12	0.494	0.134	0.134	0.034	0.132	0.033	0.030	0.009
16	0.683	0.097	0.093	0.013	0.088	0.013	0.013	0
18	0.818	0.056	0.058	0.003	0.055	0.005	0.004	0
28	0.042	0.092	0.089	0.149	0.093	0.166	0.115	0.254
39	0.294	0.155	0.150	0.070	0.161	0.070	0.065	0.036
19	0.343	0.154	0.152	0.060	0.168	0.027	0.069	0.026
41	0.456	0.140	0.139	0.039	0.136	0.043	0.037	0.011
20	0.584	0.117	0.117	0.021	0.111	0.028	0.017	0.006
40	0.667	0.097	0.097	0.014	0.094	0.016	0.012	0.004
21	0.763	0.075	0.072	0.006	0.073	0.004	0.006	0
22	0.896	0.033	0.034	0.001	0.034	0	0.002	0
23	0.052	0.101	0.099	0.142	0.109	0.156	0.122	0.218
42	0.239	0.152	0.147	0.083	0.177	0.069	0.088	0.045
24	0.244	0.155	0.153	0.085	0.157	0.088	0.071	0.049
44	0.480	0.136	0.134	0.034	0.139	0.003	0.034	0.009
25	0.476	0.140	0.134	0.035	0.142	0.023	0.037	0.013
43	0.714	0.086	0.086	0.009	0.086	0.009	0.009	0
26	0.706	0.091	0.085	0.010	0.083	0.012	0.014	0
27	0.875	0.039	0.040	0.001	0.037	0.005	0.002	0
45	0.142	0.135	0.138	0.122	0.144	0.121	0.104	0.094
49	0.230	0.154	0.147	0.088	0.162	0.093	0.080	0.046
46	0.443	0.140	0.140	0.042	0.139	0.048	0.037	0.011
50	0.513	0.131	0.125	0.031	0.130	0.040	0.026	0.005
47	0.577	0.118	0.118	0.022	0.115	0.025	0.018	0.008
51	0.775	0.067	0.073	0.007	0.068	0.003	0.007	0
48	0.823	0.055	0.055	0.004	0.053	0.005	0.004	0

between calculated and experimenal values of the copolymer composition. The best-fit was found by minimizing the quantity R defined by

$$R = \sum_i \left[\frac{F_E^{exp} - F_E^{calc}}{F_E^{exp}} \right]^2 \quad (3)$$

where the superscripts 'exp' and 'calc' indicate experimental and calculated values. The initial feed composition was assumed to be known with infinite precision. To take account of composition drift over a finite conversion, the copolymerization was simulated as a series of small steps. During a step the feed composition was assumed constant and the polymer composition was calculated using equation (1). After each step, the feed composition was adjusted according to the amount of each monomer which had entered the polymer and the process repeated up to the experimental conversion for that particular sample. The polymer composition was then averaged over all steps. Trial calculations with different step lengths showed that a step length of 0.2% of the initial monomer was sufficiently small.

Method II. Triad sequence distribution

For the terminal-unit copolymerization model above, the sequence statistics are governed by four first-order Markov probabilities, P(E|E), P(E|P), P(P|E) and P(P|P) where e.g. P(E|P) represents the probability that a PO monomer adds to an EO chain end. By definition, these probabilities are related by

$$P(E|E) + P(E|P) = 1$$

$$P(P|E) + P(P|P) = 1.$$

For simplicity, let

$$u = P(E|P)$$

$$w = P(P|E)$$

The instantaneous probabilities u and w are expressed in terms of the reactivity ratios and the feed composition by

$$u = 1/(r_E x + 1) \quad (4a)$$

$$w = x/(r_P + x) \quad (4b)$$

where $x = f_E/(1 - f_E)$.

Previous ^{13}C-NMR studies of the structure of poly(propylene oxide) [1, 19] have shown that PO adds overwhelmingly in a regular head-to-tail manner. Considering only this mode of addition, there are eight distinct compositional triads for which the probabilities for an infinite chain are related to u and w by

$$[EEE] = w(1-u)^2/(u+w) \quad (5a)$$

$$[EE\vec{P}] = [\vec{P}EE] = uw(1-u)/(u+w) \quad (5b)$$

$$[\vec{P}E\vec{P}] = u^2w/(u+w) \quad (5c)$$

$$[E\vec{P}E] = uw^2/(u+w) \quad (5d)$$

$$[E\vec{P}\vec{P}] = [\vec{P}\vec{P}E] = uw(1-w)/(u+w) \quad (5e)$$

$$[\vec{P}\vec{P}\vec{P}] = u(1-w)^2/(u+w). \quad (5f)$$

By definition, the sum of all triad probabilities must be unity. Furthermore the relationships

$$[\vec{P}EE] = [EE\vec{P}]$$

$$[\vec{P}\vec{P}E] = [E\vec{P}\vec{P}]$$

$$[EE\vec{P}] + [\vec{P}EE] + 2[\vec{P}E\vec{P}] = [E\vec{P}\vec{P}] + [\vec{P}\vec{P}E] + 2[E\vec{P}E]$$

must necessarily be obeyed [1], and therefore only four of the triad probabilities are in fact independent. Reactivity ratios can be obtained from the triad distribution for each copolymer using equations (4) and (5) and the feed composition parameter x for that sample. In principle, variation of the reactivity ratios with feed composition may also be monitored.

In this work, the reactivity ratios were obtained from a computer search for those values giving the best fit to the experimental triad distribution, the best fit being found by minimizing the quantity

$$S = \sum_{\text{triads}} \left[\frac{X_i^{exp} - X_i^{calc}}{X_i^{exp}} \right]^2 \quad (6)$$

where X_i is the probability of the ith triad. As in Method I drift in the feed composition during the polymerization (and hence in the probabilities u and w) was dealt with by simulating the polymerization as a series of small steps and averaging the distribution over all the steps.

RESULTS

Table 2 gives conversion, molecular weight and composition data for all the copolymers prepared. The polymer compositions are an average of values from ^{1}H- and ^{13}C-spectra; typically these differed by $<2\%$. The observed molecular weights were obtained from ^{13}C-spectra; they were of the order of one-half to two-thirds of the value expected from the initial amounts of monomers and initiator and the degree of conversion. The difference is due partly to initiation by small amounts of adventitious water and partly to a chain transfer reaction involving PO; the implications of this reaction are discussed further below.

Figure 1 shows a typical backbone ^{13}C-NMR spectrum [1]. Peaks are identified using the following notation:

(i) E and $\vec{P}$ represent —OCH_2CH_2— and —$OCH_2CH(CH_3)$— units respectively;
(ii) s and t represent CH_2 and CH carbons in a $\vec{P}$ unit;
(iii) a and b represent the left-hand and right-hand carbons in an E unit;
(iv) an end unit is represented by E* or $\vec{P}$*.

The vertically expanded region (60–68 ppm) in Fig. 1(a) demonstrates the very low intensity of end-groups. Figure 1(b) shows an expansion of the 74.5–75.5 ppm region of the CH subspectrum from which the $\vec{P}$-centred triad distribution was obtained, while Fig. 1(c) shows an expansion of the 70–71 ppm region of the CH_2 subspectrum from which the E-centred triad distribution was obtained.

Table 3 gives the best-fit reactivity ratios determined by Method I using the composition and

conversion data in Table 2. The agreement between calculated and experimental polymer compositions was excellent, with mean errors of generally $<1\%$. In order to quantify the uncertainties in the reactivity ratios, we show in Fig. 2 a contour plot of R [equation (3)] as a function of r_E and r_P for the data for 60°C. This plot shows that r_E and r_P are covariant i.e. a degradation in the quality of fit caused by changing one could be recovered to some extent by changing the other. It was not possible to derive independent uncertainty ranges for r_E and r_P. Approximately, an error of 3% in the experimental polymer compositions led to values of r_E and r_P of 2.9 ± 0.6 and 0.28 ± 0.07 respectively. Within these uncertainties, r_E and r_P for the systems catalysed by the K^+ salt were independent of temperature, with averages of 2.8 ± 0.6 and 0.25 ± 0.07 respectively.

Table 4 gives the experimental triad distributions. The uncertainties for the $\vec{P}$-centred triad probabilities were greater than those for the E-centred triads because of a difference in the procedure for transforming NMR signal intensities into triad probabilities [1]. Thus the probabilities of the E-centred triads were obtained from four well-resolved CH_2 signals, three of which are attributable to only one triad while the fourth is attributed to overlapping signals from two triads. However the probabilities of the $\vec{P}$-centred triads were obtained from four less well-resolved groups of CH peaks only one of which could be assigned solely to one triad (actually the $\vec{P}\vec{P}\vec{P}$). The other three groups arose from various combinations of the other three triads. Hence errors in the basic NMR integrations were multiplied in the calculation of the $\vec{P}$-centred triad probabilities. The effect of this more extended manipulation of the $\vec{P}$-centred triads is revealed by comparing the $E\vec{P}\vec{P}$ probabilities with the $\vec{P}\vec{P}E$ probabilities, and the $EE\vec{P}$ probabilities with the $\vec{P}EE$ probabilities. Invariably, the probabilities of the latter pair are almost equal as expected from equation (6a), whereas the probabilities of the former pair are less consistent, in some samples being more or less equal as expected from equation (6b), but in others differing significantly. In the determination of r_E and r_P, the values of $[E\vec{P}\vec{P}]$ and $[\vec{P}\vec{P}E]$ were averaged.

In the samples with higher E content, the $\vec{P}\vec{P}\vec{P}$ triad probability was too low to measure with any confidence and hence was excluded from the fitting algorithm.

Table 5 gives the best-fit reactivity ratios from the triad-fitting procedure. For the vast majority of samples, the RMS error in the fitted data was satisfactory at 5% or less. The uncertainties in the ratios depended on the overall composition, being lower for samples with reasonably high probabilities of all triads ($F_E \leqslant \approx 0.8$) than for samples where some triads were of very low probability. In particular, the value of r_P was not determined accurately when F_E was high because of the relatively unreliable values of the probabilities of triads involving the $\vec{P}\vec{P}$ sequence. As in the case of the composition fitting by Method I above, it was not possible to derive independent uncertainties in r_E and r_P. An example of a contour plot of the sum of fractional deviations, S, as a function of r_E and r_P is shown for a mid-range sample in Fig. 3. An upper limit of 10% in the experimental error for the triad probabilities, corresponding to a value for S of 0.08, led to intervals of about ± 0.4 for r_E and ± 0.04 for r_P. Similar plots were used to show

Table 5. Best-fit reactivity ratios from the triad distribution in Table 4 (Method II)

T (°C)	Counterion	Sample	r_E	r_P	RMS error (%)
0	K^+	34	3.2	0.27	7.0
		35	3.2	0.28	5.9
		36	3.2	0.29	1.4
		37	3.3	0.31	3.4
		38	3.0	0.51	2.0
23	K^+	29	3.1	0.27	5.6
		30	3.0	0.30	2.0
		31	3.1	0.30	5.5
		32	3.0	0.31	1.1
		33	3.0	0.49	4.2
40	K^+	11	3.1	0.26	6.6
		17	2.9	0.30	3.9
		12	3.1	0.30	1.5
		16	3.0	0.34	2.5
		18	3.0	0.45	3.1
60	K^+	28	3.0	0.29	5.7
		39	3.0	0.32	4.8
		19	3.2	0.28	11.7
		41	3.0	0.32	2.5
		20	3.1	0.34	2.5
		40	3.0	0.34	1.2
		21	3.1	0.27	3.5
		22	3.0	0.31	3.3
80	K^+	23	3.1	0.28	6.7
		42	3.0	0.30	5.9
		24	3.0	0.31	4.2
		44	3.0	0.32	3.0
		25	3.1	0.33	13.8
		43	3.0	0.31	2.0
		26	3.0	0.44	3.3
		27	3.0	0.80	5.9
40	Na^+	45	3.4	0.26	1.9
		49	3.2	0.27	3.1
		46	3.2	0.29	3.0
		50	3.0	0.27	10.6
		47	3.2	0.29	1.5
		51	2.9	0.28	4.2
		48	3.1	0.44	0.5

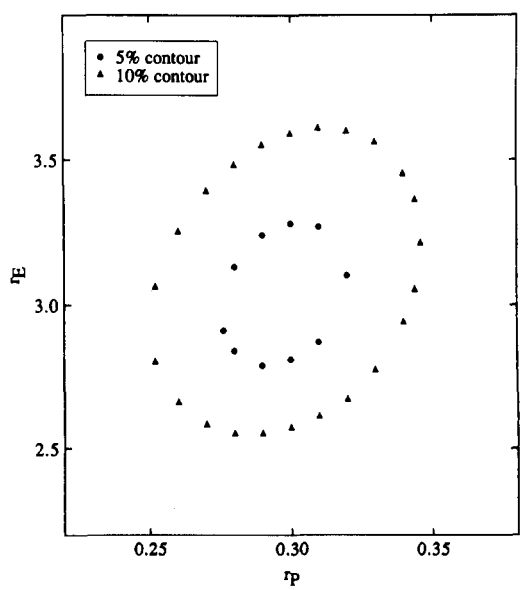

Fig. 3. Contour plot of the error sum S [equation (6)] as a function of r_E and r_P for sample 30.

that for $f_E \geqslant \approx 0.8$, the uncertainty range for r_P increases to about ± 0.08. Within these limits, r_E was independent of feed composition, counterion and temperature, averaging 3.1 ± 0.4 in excellent agreement with the value from Method I above. r_P was also independent of counterion and temperature, and of composition below $f_E \approx 0.8$ with an average value of 0.30 ± 0.04 which is also in good agreement with the value from Method I. However higher values of r_P were found for $f_E > \approx 0.8$, though the results were somewhat erratic.

DISCUSSION

It is gratifying that the reactivity ratios obtained from the copolymer composition and from the sequence distribution on the whole agree within experimental error. Evidently the precautions taken to avoid errors due to composition drift during the copolymerization (by using a numerical integration procedure) and end-groups (by preparing high molecular weight samples) proved largely successful.

It is not clear whether the tendency for the best-fit value of r_P to rise at high F_E values is real. For these samples, the triads containing the $\bar{P}\bar{P}$ dyad, which are critical in determining r_P, are detectable but of extremely low probability. It is possible that small systematic errors distort the intensities of these triads in this composition regime. It is worth pointing out that the overall copolymer composition can be accurately measured over the whole composition range, but no systematic variations in quality of the composition fit were observed at high f_E.

One possible source of error not yet considered is a chain transfer reaction in the anionic polymerization of PO which is believed to involve the formation of allyl groups and the initiation of new chains according to the following mechanism [20–25]:

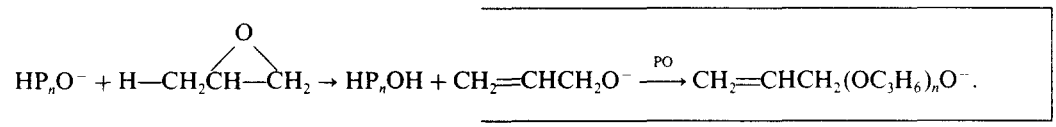

$$HP_nO^- + H{-}CH_2\underset{\diagdown\,O\,\diagup}{CH}{-}CH_2 \rightarrow HP_nOH + CH_2{=}CHCH_2O^- \xrightarrow{PO} CH_2{=}CHCH_2(OC_3H_6)_nO^-.$$

This reaction is one reason for the discrepancy between the observed molecular weight and that predicted from the initial amounts of monomer and initiator and the conversion. The extent of transfer can be monitored either by ^{13}C- [19] or ^1H- [26] NMR via the distinct olefinic resonances. In the present work, the fraction of *polymerized* PO monomer incorporated as allyl groups was found to be quite small, varying from *ca* 0.005 at 0°C to *ca* 0.025 at 80°C. At such low levels, the transfer has no significant effect on the determination of reactivity ratios.

The values of r_E and r_P indicate that EO monomer polymerizes more rapidly than PO. The product $r_E r_P$ is 0.9 i.e. very close to the value of unity which characterizes ideal copolymerization when the chain-end has no influence on the probability of adding EO or PO. Thus the relative preference for EO addition is determined by a difference in monomer reactivity rather than chain-end reactivity. In particular there does not appear to be any significant additional hindrance to PO addition from steric interaction between CH_3 side-groups. This is consistent with the perfectly atactic structure of anionically catalysed PPO [1], since any inter-methyl interaction would be expected to favour either isotactic or syndiotactic addition. The finding that r_E and r_P are unaltered when the cation is changed from K^+ to Na^+ is additional evidence of the insensitivity of the addition probabilities to the chain-end.

Acknowledgements—The authors thank the SERC for a grant towards the purchase of the NMR spectrometer, and ICI Ltd for a research studentship for GEY.

REFERENCES

1. F. Heatley, Y.-Z. Luo, J.-F. Ding, R. H. Mobbs and C. Booth. *Macromolecules* **21,** 2713 (1989).
2. C. Campbell, F. Heatley, G. Holcroft and C. Booth. *Eur. Polym. J.* **25,** 831 (1989).
3. F. Heatley, G.-E. Yu, W.-B. Sun, E. J. Pywell, R. H. Mobbs and C. Booth. *Eur. Polym. J.* **26,** 583 (1990).
4. F. Heatley, G.-E. Yu, M. D. Draper and C. Booth. *Eur. Polym. J.* **27,** 471 (1991).
5. S. Kolosow. Diplomarbeit TU, Dresden (1975) [quoted in H. Becker, G. Wagner and A. Stolarzewicz. *Acta Polym.* **32,** 764 (1981)].
6. A. Stolarzewicz, H. Becker and G. Wagner. *Acta Polym.* **31,** 743 (1980).
7. G. Heublein, R. Wondraczek, H. Toparkus and H. Berndt. *Faserforsch. Textiltechnik* **26,** 537 (1975); *Z. Polymerforsch.* **27,** 57 (1976).
8. G. A. Gladkovskij. Dissertation, Vsesojuznij Naueij Institut Issledovanija Sinteticeskich Smol, Vladimir, 1974 (quoted in Ref. [6]).
9. A. K. Rastogi and L. E. St. Pierre. *J. appl. Polym. Sci.* **14,** 1179 (1970).
10. M. Fineman and D. J. Ross. *J. Polym. Sci.* **5,** 259 (1950).
11. C. M. Boussias. M.Sc. Thesis, University of Manchester (1974).
12. V. A. Ponomarenko, A. M. Khomutov, S. J. Ilchenko and A. V. Ignatenko. *Polym. Sci. USSR* **13,** 1735 (1971).
13. G. A. Gladovskii and Ye. V. Ryzhenkova. *Polym. Sci. USSR* **13,** 723 (1971).
14. D. M. Doddrell, D. T. Pegg and M. R. Bendall. *J. Chem. Phys.* **77,** 2745 (1982).
15. T. Alfrey and G. Goldfinger. *J. Chem. Phys.* **12,** 205 (1944).
16. F. R. Mayo and F. M. Lewis. *J. Am. chem. Soc.* **66,** 1594 (1944).
17. F. T. Wall. *J. Am. chem. Soc.* **66,** 2050 (1944).
18. V. E. Meyer and G. G. Lowry. *J. Polym. Sci., Part A* **3,** 2843 (1965).
19. F. C. Schilling and A. E. Tonelli. *Macromolecules* **19,** 1337 (1986).
20. L. E. St. Pierre and C. C. Price. *J. Am. chem. Soc.* **78,** 3432 (1956).
21. D. M. Simons and J. H. Verbanc. *J. Polym. Sci.* **44,** 303 (1960).
22. G. Gee, W. C. E. Higginson, K. J. Taylor and M. W. Trenholme. *J. Chem. Soc.* 4298 (1961).
23. W. H. Snyder Jr. Ph.D. Thesis, University of Pennsylvania (1961).
24. C. C. Price and D. D. Carmelite. *J. Am. chem. Soc.* **88,** 4039 (1966).
25. G. A. Gladkovskii, L. P. Golovina, G. F. Vedeneyeva and V. S. Lebedev. *Polym. Sci. USSR* **15,** 1370 (1973).
26. J.-F. Ding. Ph.D. Thesis, University of Manchester (1990).